Hindawi Publishing Corporation
International Journal of Photoenergy
Volume 2013, Article ID 289290, 11 pages
http://dx.doi.org/10.1155/2013/289290

Research Article

Intensification of Azo Dye Removal Rate in the Presence of Immobilized TiO_2 Nanoparticles and Inorganic Anions under UV-C Irradiation: Optimization by Response Surface Methodology

Mohammad A. Behnajady and Mahsa Hajiahmadi

Department of Chemistry, Faculty of Science, Tabriz Branch, Islamic Azad University, Tabriz 5157944533, Iran

Correspondence should be addressed to Mohammad A. Behnajady; behnajady@iaut.ac.ir

Received 28 May 2013; Revised 14 August 2013; Accepted 4 September 2013

Academic Editor: Peter Robertson

Wastewaters contain inorganic anions that affect the removal rate of organic pollutants. The present study aims to optimize the effects of inorganic anions such as NO_3^-, Cl^-, HCO_3^-, and $H_2PO_4^-$ on the removal rate of an organic pollutant in the presence of immobilized TiO_2 nanoparticles using response surface methodology (RSM). C.I. Acid Red 17 (AR17) was used as a model organic pollutant. Thirty experiments were required to study the effects of anions in various concentrations. The results indicate that the addition of NO_3^- and HCO_3^- ions intensifies the removal rate of AR17. The results of the analysis of variance (ANOVA) showed a high coefficient of determination value ($R^2 = 0.9866$ and $R_{adj.}^2 = 0.9822$). The results indicate that RSM is a suitable method for modeling and optimizing the process. The results prove that in the presence of and NO_3^- and HCO_3^- ions especially in the combination situation the removal rate of AR17 is enhanced considerably. An important synergy effect was observed in the combination of NO_3^- and HCO_3^- ions, so that AR17 removal percent under the optimized RSM conditions was considerably more than the sum of removal percent when these ions are used individually.

1. Introduction

Producing many products such as clothes, leather accessories, and furniture, needs synthetic dyes. Most of these dyes are toxic and potentially carcinogenic in nature. The discharge of their effluents into the environment is harmful for human and all living beings. Therefore, their removal from industrial effluents is considered as a major concern and responsibility [1–4]. Azo dyes are the largest group of commercial dyes [5]. Among the various treatment methods, advanced oxidation processes (AOPs) have been reported as a promising and practical method [2, 6, 7]. Heterogeneous photocatalysis is one of the AOPs and has attracted extensive attention of many researchers. This method is based on producing photoexcited electrons (e^-) in the conduction band and positive-charged holes (h^+) in the valence band of an oxide semiconductor like TiO_2 under ultraviolet (UV) light. The valence band holes are powerful oxidants, and the conduction band electrons are great reductants. Reactions include oxidation of organic pollutants by photogenerated positive holes (h^+) or by reactive oxygen species ($HO^\bullet$, $HOO^\bullet$, and $O_2^{\bullet-}$) formed on the TiO_2 surface under UV light irradiation [8–10].

Dye-containing wastewaters have inorganic anions such as nitrate, chloride, bicarbonate, sulfate, and dihydrogenphosphate that impress removal rate of pollutants. Most of the investigations have reported inhibitory effects of inorganic anions on the removal rate of pollutants in the AOPs [11–15].

Response surface methodology (RSM) is a statistical method to reduce the number of the experiments. Mathematical and statistical techniques are applied in this method

Table 1: Structure and characteristics of C.I. Acid Red 17 (AR17).

Chemical structure	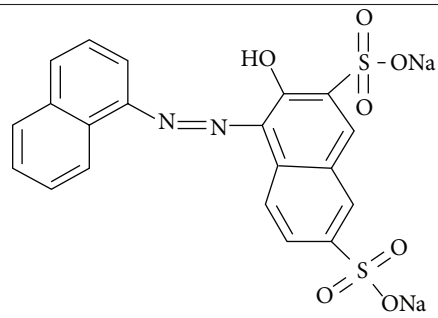
Chemical formula	$C_{20}H_{12}N_2Na_2O_7S_2$
M_w (g mol^{-1})	502.41
λ_{max} (nm)	518
C.I. number	16180

to analyze the effect of the independent variables (inorganic anions concentration) on a specific dependent variable (removal percent). This method gives linear interaction and quadratic effects of the factors and is useful for the optimization of process [16, 17]. In this paper, $NaNO_3$, $NaHCO_3$, NaH_2PO_4, and NaCl were used as additives, and the effects of these anions on the removal of the model dye pollutant in the presence of immobilized TiO_2 nanoparticles on a glass plate were investigated and optimized via using response surface methodology.

2. Materials and Methods

2.1. Materials. C.I. Acid Red 17 (AR17) was used as a model pollutant. It is a monoazo dye of acid class and was obtained from ACROS Co. Its chemical structure and other characteristics are illustrated in Table 1. Titanium dioxide (P25, ca. 80% anatase, 20% rutile; BET area, ca. 50 m^2 g^{-1}; mean particle size, ca. 21 nm; containing 99.5% TiO_2) was supplied by Degussa Co., and $NaNO_3$, NaCl, $NaHCO_3$, and NaH_2PO_4 were obtained from Merck Co. and were used without further purification. N,N-dimethyl-*p*-nitroso-aniline was purchased from Fluka (Switzerland).

2.2. Immobilization of TiO_2-P25 on Glass Plates. Heat attachment method was used to prepare the immobilized TiO_2-P25 on glass plate (1.5 × 18 cm^2) [18]. To obtain immobilized TiO_2, a suspension containing 10 g L^{-1} TiO_2-P25 in double distilled water was prepared. Then, its pH was adjusted to about 1.5 by HNO_3. The prepared suspension was sonicated in an ultrasonic bath (Elma, Windaus T460/H, Germany) under frequency of 35 kHz for 30 min in order to improve the dispersion of TiO_2-P25 in water. Glass plate was treated with a diluted HF solution (5% v/v) in order to make a rough surface for better contact with TiO_2 nanoparticles. The treated glass plate was washed with double distilled water several times. Next, sonicated TiO_2 suspension was poured on glass plate for 20 min, then removed from the suspension, and then placed in an oven at 150°C. After drying, the glass plate was heated at 500°C in a furnace for 2 h and then was thoroughly washed with double distilled water to remove the poorly attached or free TiO_2 particles [19, 20]. The deposition process was carried out twice to increase the loaded TiO_2 on the surface of glass plate. Typically, the deposited TiO_2 is 0.26 mg cm^{-2}. The characteristics of the TiO_2 nanoparticles immobilized on the glass plate were determined using an atomic force microscopy (AFM) carried out by DME (Danish Micro Engineering A/S).

2.3. Photoreactor and Light Source. A cylindrical quartz reactor of 100 mL capacity at batch mode containing a gas disperser at the bottom of the reactor was used for the removal of AR17 under UV-C light irradiation. The radiation source was a UV lamp (15 W, UV-C, λ_{max} = 254 nm, manufactured by Philips), which was placed in front of the cylindrical quartz reactor. The glass plate, coated with titanium dioxide nanoparticles as a catalyst, was positioned inside the cylindrical quartz reactor in front of the UV lamp [21].

2.4. Procedures. Stock solutions for AR17 and each inorganic anion were prepared with double distilled water and diluted to various concentrations in the experiments. A solution containing AR17 (30 mg L^{-1}) and various concentrations of aforementioned anions were prepared, and then 100 mL of the prepared solution was transferred into the cylindrical quartz reactor until the catalyst was completely immersed in the solution. It was continuously purged with O_2 through a gas disperser, 30 min before the irradiation and during the irradiation time for saturation of the solution with oxygen. Samples were pulled out from the reactor after 5 min irradiation, and the absorbance of AR17 was measured by means of a UV-Vis spectrophotometer (Ultrospec 2000, Biotech Pharmacia, England) at 518 nm. The light intensity of the light source was measured using Lux-UV-IR meter (Leybold Co., GmbH), and typically it was 42 W m^{-2}.

2.5. Central Composite Design. The useful design for fitting second-order models is Central Composite Design (CCD) proposed by Box and Wilson in 1951 and has attracted extensive attention [22, 23]. The CCD combines a two-level full/fractional factorial design with additional star points and minimum one point at the center of the experimental position. The required experiment numbers in the CCD is computed using the following equation:

$$N = 2^k + 2k + C_0, \tag{1}$$

where k is the number of factors and C_0 is the replication numbers of central point. In this design, all factors are studied at five levels [22, 24]. In addition, in the CCD the variable parameters, that is, X_i, were coded as x_i. For this purpose, the following relationship was used:

$$x_i = \frac{X_i - X_0}{\delta X}, \tag{2}$$

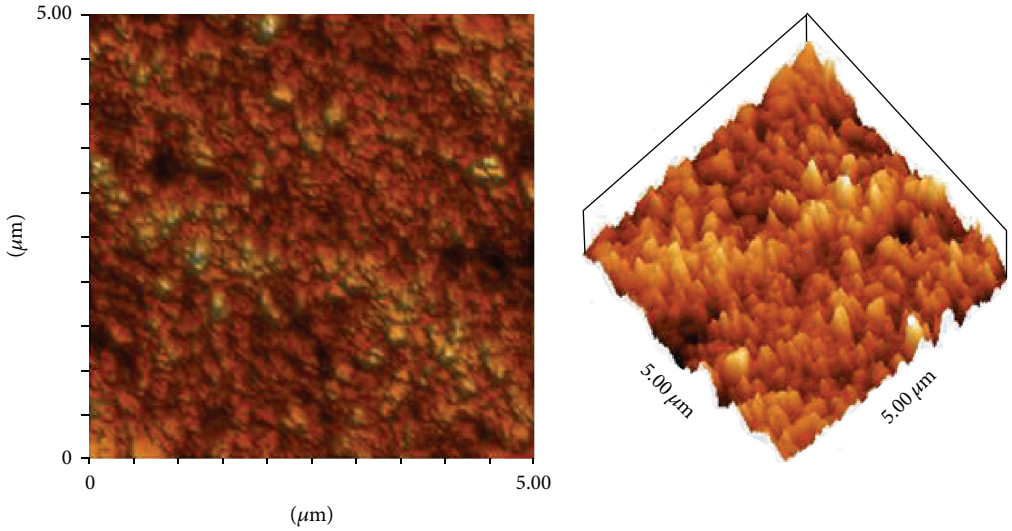

Figure 1: Two- and three-dimensional AFM images of TiO_2-P25 nanoparticles immobilized on glass plate.

Table 2: Experimental ranges and levels of the independent test variables.

Variables	Ranges and levels				
	−2	−1	0	+1	+2
NO_3^- concentration (mM)	0	30	60	90	120
HCO_3^- concentration (mM)	0	30	60	90	120
$H_2PO_4^-$ concentration (mM)	0	30	60	90	120
Cl^- concentration (mM)	0	30	60	90	120

Table 3: Morphological information of TiO_2-P25 nanoparticles immobilized on glass plate.

Projected area (μm^2)	RMS roughness (nm)	Average roughness (nm)	Surface skewness (Ssk)	Surface kurtosis (Sku)
25	37.1	28.9	0.43	3.76

where X_0 is the value of X_i in the central point and δX represents the step change [25, 26]. In the present study, the concentrations of NO_3^-, HCO_3^-, $H_2PO_4^-$, and Cl^- ions were determined in terms of four main factors in order to evaluate the effects of these inorganic anions on the removal efficiency of AR17. Totally, 30 experiments were carried out including six replications in the central point. The experimental ranges and the levels of the independent variables for AR17 removal are provided in Table 2. The experimental data were analyzed using DX7 software.

3. Results and Discussion

3.1. Atomic Force Microscopy (AFM) of TiO_2-P25 Immobilized on Glass Plate. Figure 1 shows two- and three-dimensional AFM pictures of TiO_2-P25 nanoparticles immobilized on glass plate for a projected area of $5 \times 5\,\mu m^2$. The results of AFM (Table 3) allow making a morphological interpretation of the catalyst surface. The results indicate the formation of a surface with root mean square (RMS) and average roughness of 37.1 and 28.9 nm, respectively. The surface skewness (Ssk) describes the asymmetry of the height distribution histogram. Ssk = 0 indicates a symmetric height distribution like a Gaussian. The surface kurtosis (Sku) is another parameter used to describe the surface topography. For Gaussian height distribution, Sku approaches 3.0 whereas the lower values indicate broader height distribution [27]. The values of Ssk and Sku for the prepared catalyst surface indicate a fairly symmetric height distribution of Gaussian.

3.2. Central Composite Design Model. The present study made use of Central Composite Design (CCD) for the optimization of AR17 removal rate in the presence of various concentrations of inorganic anions. The structure of this design and the results of the measurement of AR17 removal percent after 5 min irradiation are shown in Table 4. In order to correlate the dependent and independent variables, the following second-order polynomial response equation was used:

$$\begin{aligned} Y &= b_0 + b_1x_1 + b_2x_2 + b_3x_3 + b_4x_4 \\ &\quad + b_{12}x_1x_2 + b_{13}x_1x_3 + b_{14}x_1x_4 \\ &\quad + b_{23}x_2x_3 + b_{24}x_2x_4 + b_{34}x_3x_4 \\ &\quad + b_{11}x_1^2 + b_{22}x_2^2 + b_{33}x_3^2 + b_{44}x_4^2, \end{aligned} \tag{3}$$

where Y is AR17 removal percent after 5 min irradiation (response variable), b_i is regression coefficient for linear effects, b_{ii} is regression coefficient for squared effects, b_{ik} is regression coefficient for interaction effects, and x_i is the coded experimental level of the variables.

According to this design, an empirical reduced quadratic relationship with significant model terms between the removal efficiency of AR17 (response, Y) and inorganic ions

Table 4: The four-factor central composite design matrix and the value of the response function (R%).

Run	$[NO_3^-]$ (mM)	$[HCO_3^-]$ (mM)	$[H_2PO_4^-]$ (mM)	$[Cl^-]$ (mM)	Removal efficiency (%)	
					Experimental	Predicted
1	−1	−1	−1	−1	34.394	35.180
2	1	−1	−1	−1	61.432	65.392
3	−1	1	−1	−1	51.023	48.756
4	1	1	−1	−1	85.646	88.019
5	−1	−1	1	−1	28.299	27.683
6	1	−1	1	−1	48.023	49.524
7	−1	1	1	−1	36.013	32.998
8	1	1	1	−1	63.727	63.892
9	−1	−1	−1	1	35.902	35.180
10	1	−1	−1	1	65.375	65.392
11	−1	1	−1	1	48.998	48.756
12	1	1	−1	1	88.119	88.019
13	−1	−1	1	1	29.110	27.683
14	1	−1	1	1	48.287	49.524
15	−1	1	1	1	33.731	32.998
16	1	1	1	1	63.892	63.892
17	−2	0	0	0	5.887	10.120
18	2	0	0	0	75.686	71.225
19	0	−2	0	0	42.957	41.045
20	0	2	0	0	66.262	68.988
21	0	0	−2	0	75.474	70.829
22	0	0	2	0	40.503	39.204
23	0	0	0	−2	54.416	55.016
24	0	0	0	2	53.965	55.016
25	0	0	0	0	53.066	55.016
26	0	0	0	0	55.525	55.016
27	0	0	0	0	55.066	55.016
28	0	0	0	0	54.268	55.016
29	0	0	0	0	55.147	55.016
30	0	0	0	0	54.591	55.016

concentration (variable parameters) was obtained using the following formula:

$$Y = 55.02 + 15.28x_1 + 6.99x_2 - 7.91x_3 + 2.26x_1x_2 - 2.09x_1x_3 - 2.06x_2x_3 - 3.59x_1^2, \quad (4)$$

where x_1, x_2, and x_3 represent the NO_3^-, HCO_3^-, and $H_2PO_4^-$ concentrations, respectively. The results show that a quadratic response surface model fits the process. The predicted removal efficiencies by (4) are provided in Table 4. The results show that there are perfect agreements between the experimental and predicted values of removal efficiency. According to (4), the effective parameters in this process include NO_3^- concentration, HCO_3^- concentration, $H_2PO_4^-$ concentration, mutual effects of NO_3^- and HCO_3^- concentration, NO_3^- and $H_2PO_4^-$ concentration, HCO_3^- and $H_2PO_4^-$ concentration, and the square effect of NO_3^- concentration. Furthermore, according to the model, Cl^- concentration was considered as an ineffective factor.

The measurement of the residuals is a method to evaluate the adequacy of the model where the residuals represent the differences between the observed and the predicted response values. Normal probability plot is a suitable graphical method to know about the normality of the residuals. As shown in Figure 2, the inclination of the residuals is towards normal distribution. Figure 2 shows that the residuals in the plot rise and fall randomly around the central line. These two plots revealed that the model is adequate for explaining the process under study.

ANOVA was used to study the significance and adequacy of the model. The correlation coefficient (R^2) value is a standard value to know how much variability in the observed response values can be explained by the experimental factors and their interactions. The results show a high value of coefficient of determination ($R^2 = 0.9866$ and $R_{\text{adj.}}^2 = 0.9822$).

Table 5: Analysis of variance (ANOVA) for fit of removal efficiency from central composite design.

Source of variations	Sum of squares	Degree of freedom	Variance	F-value	Prob. > F	
Model	8862.63	7	1266.09	230.70	<0.0001	Significant
A	5600.73	1	5600.73	1020.56	<0.0001	
B	1171.20	1	1171.20	213.41	<0.0001	
C	1500.17	1	1500.17	273.36	<0.0001	
AB	81.94	1	81.94	14.93	0.0008	
AC	70.05	1	70.05	12.76	0.0017	
BC	68.22	1	68.22	12.43	0.0019	
A^2	370.33	1	370.33	67.48	<0.0001	
Residual	120.73	22	5.49			
Lack of fit	116.90	17	6.88	8.96	0.0118	Not significant
Pure error	3.84	5	0.77			
Cor total	8983.37	29				

$R^2 = 0.9866$ and $R^2_{\text{adj.}} = 0.9822$.

This implies that 98.66% of the variations for AR17 removal efficiency can be explained by the independent variables in the represented model. However, 1.34% of variation cannot be explained by the model. Table 5 shows the results of the reduced quadratic response surface model fitting in the form of ANOVA for the removal of AR17. The variation of the model and the experimental error constitute the total variation of the results. ANOVA shows whether the variation of the model is significant in comparison with the variation of residual error or not. For this purpose, the ratio between the mean square of the model and the residual error (F-value) was used [16, 17, 28, 29]. The obtained F-value (230.70) is obviously greater than the F-value for LOF (8.96) which confirms the appropriateness of the model.

3.3. Effect of Variables as Response Surface and Contour Plots. Three-dimensional (3D) surfaces and two-dimensional (2D) contour plots, based on the model polynomial function, were drawn to investigate the effects of the inorganic anions within the range considered. Figure 3 shows the effect of NO_3^- and HCO_3^- concentration on the AR17 removal efficiency (R) for $H_2PO_4^-$ and Cl^- concentration of 60 mM. Apparently, the removal efficiency increased as NO_3^- and HCO_3^- concentration increased. However, the effect of HCO_3^- was less than the effect of NO_3^-. In order to gain approximately 80% removal efficiency, the concentration of these ions should increase up to 100 mM. Thus, it is practical to achieve the maximum removal efficiency by providing the maximum concentration of these ions. As can be seen in Figure 3, increasing the removal efficiency of the process due to increasing HCO_3^- concentration is less significant in comparison to the increasing of NO_3^- concentration which indicates that the increasing effect of NO_3^- concentration had more contribution than the increasing effect of HCO_3^- concentration.

Figure 4 shows the effect of NO_3^- and $H_2PO_4^-$ concentration on the removal efficiency (R) for HCO_3^- and Cl^- concentration of 60 mM. As it is shown in this figure, the removal efficiency increased with increasing NO_3^- concentration and decreased with increasing $H_2PO_4^-$ concentration. It is obvious that in order to achieve the maximum removal efficiency, NO_3^- concentration should be maximized and $H_2PO_4^-$ concentration should be minimized. The results indicate that the reduction effect of $H_2PO_4^-$ concentration had less contribution than the increasing effect of NO_3^- concentration.

Figure 5 shows the effect of HCO_3^- and $H_2PO_4^-$ concentration on the removal efficiency (R) for NO_3^- and Cl^- concentration of 60 mM. It is apparent that the removal efficiency increased with increasing HCO_3^- concentration and decreased with increasing $H_2PO_4^-$ concentration. Hence, the maximum removal efficiency is achieved by providing the maximum HCO_3^- and the minimum $H_2PO_4^-$ concentration.

The effects of aforementioned anions on the removal efficiency of AR17 in the presence of immobilized TiO_2 under UV-C irradiation can be explained as follows.

Apparently, the two possible effects of inorganic ions on the photocatalytic reactions are the increase of the ionic strength of the reaction medium and the scavenging of the reactive species such as hydroxyl radicals [30]. Scavenging of reactive species by inorganic anions causes an inhibitory effect in the photocatalytic activity. The increase of the ionic strength has positive effect on enhancing the photocatalytic activity. The enhancement of the removal efficiency with increasing of NO_3^- and HCO_3^- ions concentration in the fixed-bed system indicates that the reinforcement of the ionic strength of the solution in the immobilized system is more significant than their inhibitory effects. The increase of ionic strength of solution and charge transfer in fixed-bed system reduce the mass transfer limitations in this medium and increase the surface contacts between the pollutant and catalyst surface, resulting in suitable medium for removal of AR17 [13].

In the literature, three various roles for NO_3^- ions in the heterogeneous photocatalysis process have been reported. The reduction of UV light absorption by TiO_2 due to NO_3^- ions inner filter affects, and adsorption of NO_3^- ions onto TiO_2 surface causes the decreasing of adsorption and

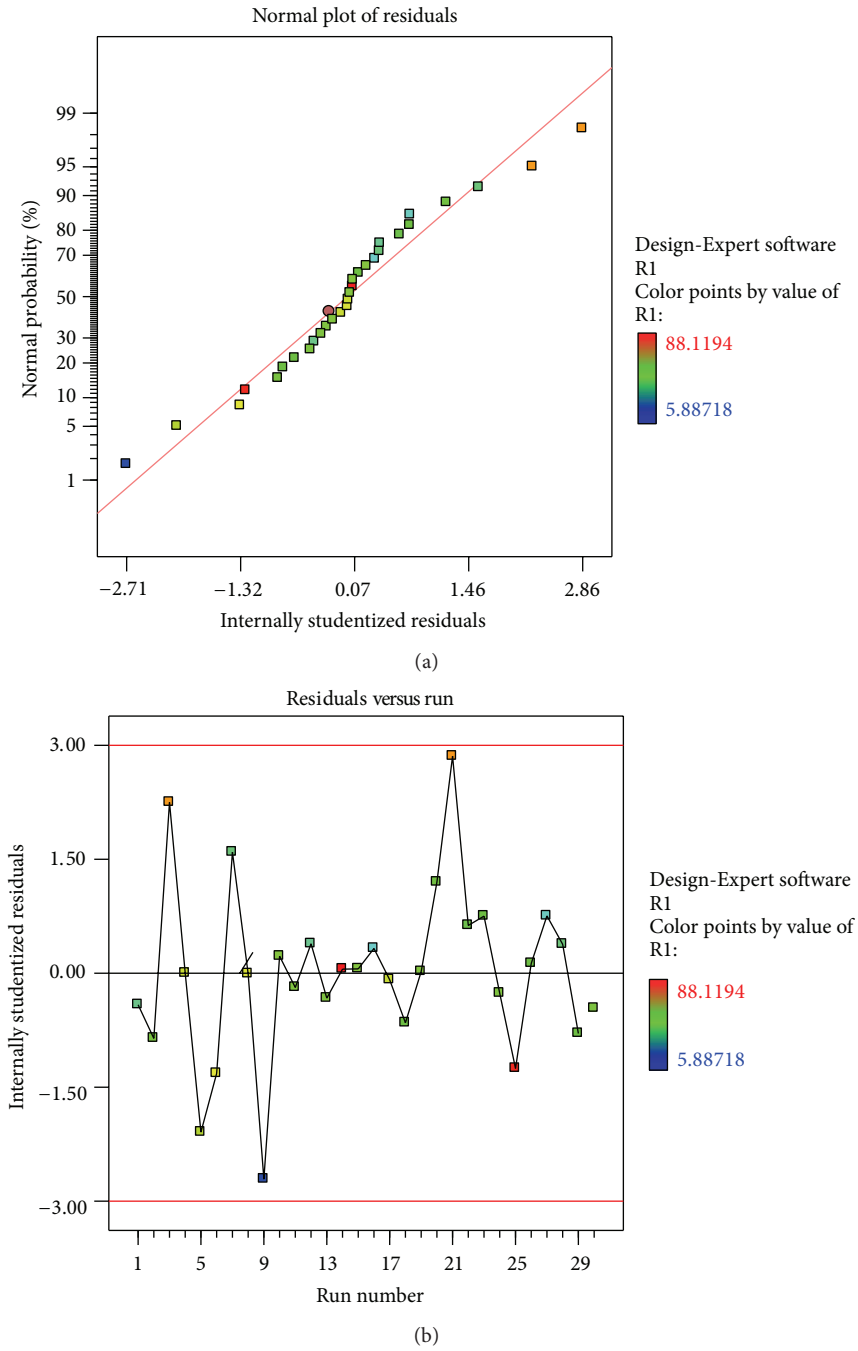

Figure 2: Residual plots for removal of AR17 in the presence of various concentrations of inorganic anions.

the contact of substrate with active sites on the catalyst surface and finally the production of hydroxyl radials according to the following equations [13, 31, 32]:

$$NO_3^- + h\upsilon \longrightarrow NO_2^- + O \quad (5)$$

$$NO_3^- + H_2O + h\upsilon \longrightarrow NO_2^{\bullet} + OH^- + HO^{\bullet} \quad (6)$$

$$O + H_2O \longrightarrow 2HO^{\bullet} \quad (7)$$

$$2NO_2^{\bullet} + H_2O \longrightarrow NO_2^- + NO_3^- + 2H^+ \quad (8)$$

In an immobilized catalyst surface, which has been tested in this study, adsorption process can be neglected due to low accessible active sites. In other words, in fixed-bed system under UV-C irradiation the increase of ionic strength of the solution and especially producing hydroxyl radials in the bulk solution according to (5)–(8) are main reasons that lead to a very high removal efficiency in the presence of NO_3^- ions. Selvam et al. [33] indicated that the presence of NO_3^- and SO_4^{2-} accelerates the removal rate of 4-fluorophenol in UV/TiO_2 process. These authors assumed that SO_4^{2-} ion

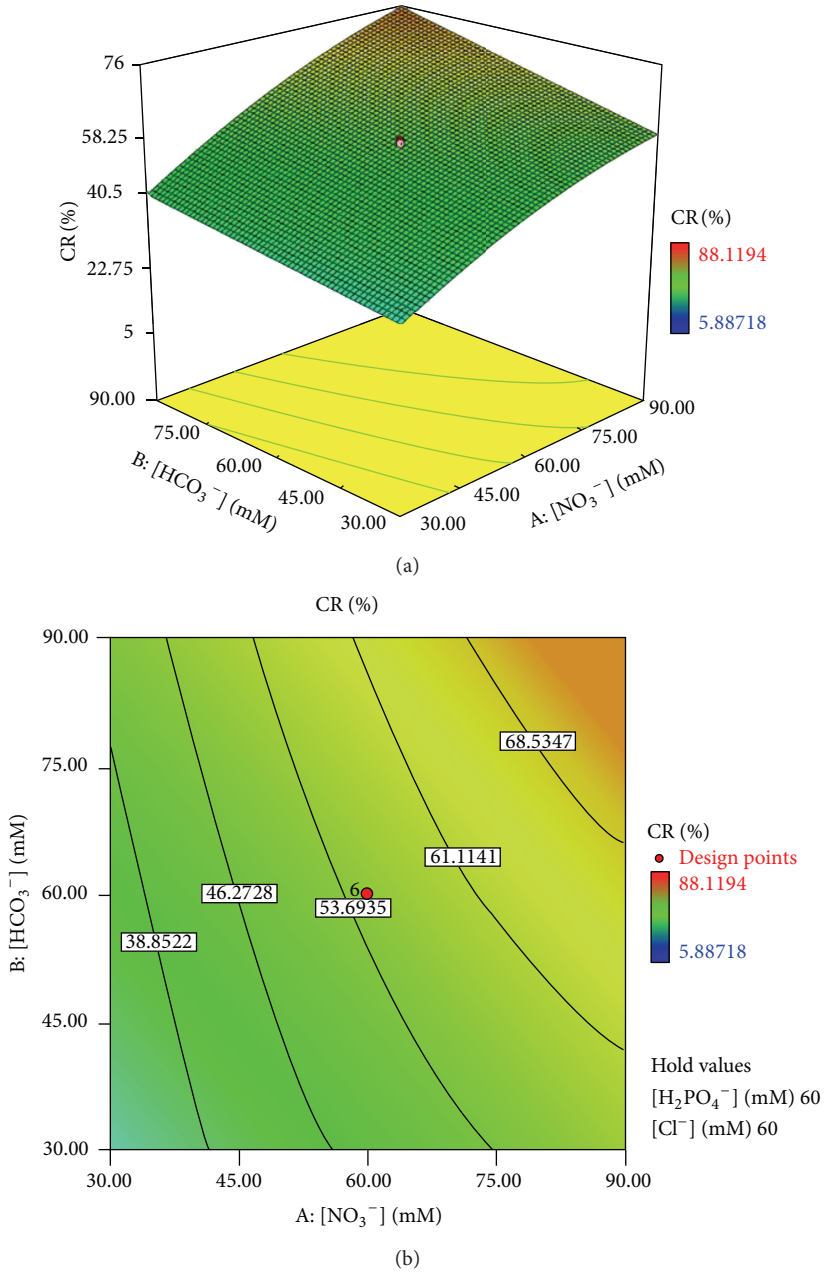

Figure 3: Response surface (a) and contour plots (b) of the removal efficiency (%) as a function of NO_3^- and HCO_3^- concentration.

reacts with hydroxyl radical to form $SO_4^{\bullet-}$ ions which can accelerate the reaction, and no hydroxyl radical quenching was reported for NO_3^- ion. Zhang et al. [13] reported that the photocatalytic degradation of reactive Brilliant Orange K-R in the packed-bed reactor increased at higher concentrations of NO_3^- ions. This effect is attributed to the formation of hydroxyl radicals from interaction of NO_3^- with UV light, and the excess free NO_3^- would also enhance charge transfer in the packed-bed reactor.

The main role of bicarbonate ions on the AOPs is that these ions are scavenger for hydroxyl radicals according to (9) [34]:

$$HCO_3^- + HO^\bullet \longrightarrow CO_3^{\bullet-} + H_2O \quad (9)$$

Bicarbonate ions can have an inhibitory or enhancing effect on the photocatalytic reactions depending on the oxidizability of substances. In the case of easily oxidizable substances, bicarbonate ions can have enhancing effect on the removal rate. It means that degradation of these substances which do not need strong oxidizing conditions can be supplied by $CO_3^{\bullet-}$ radicals [34]. Aleboyeh et al. [35] studied the effect of dyeing auxiliaries on UV/H_2O_2 removal of Acid

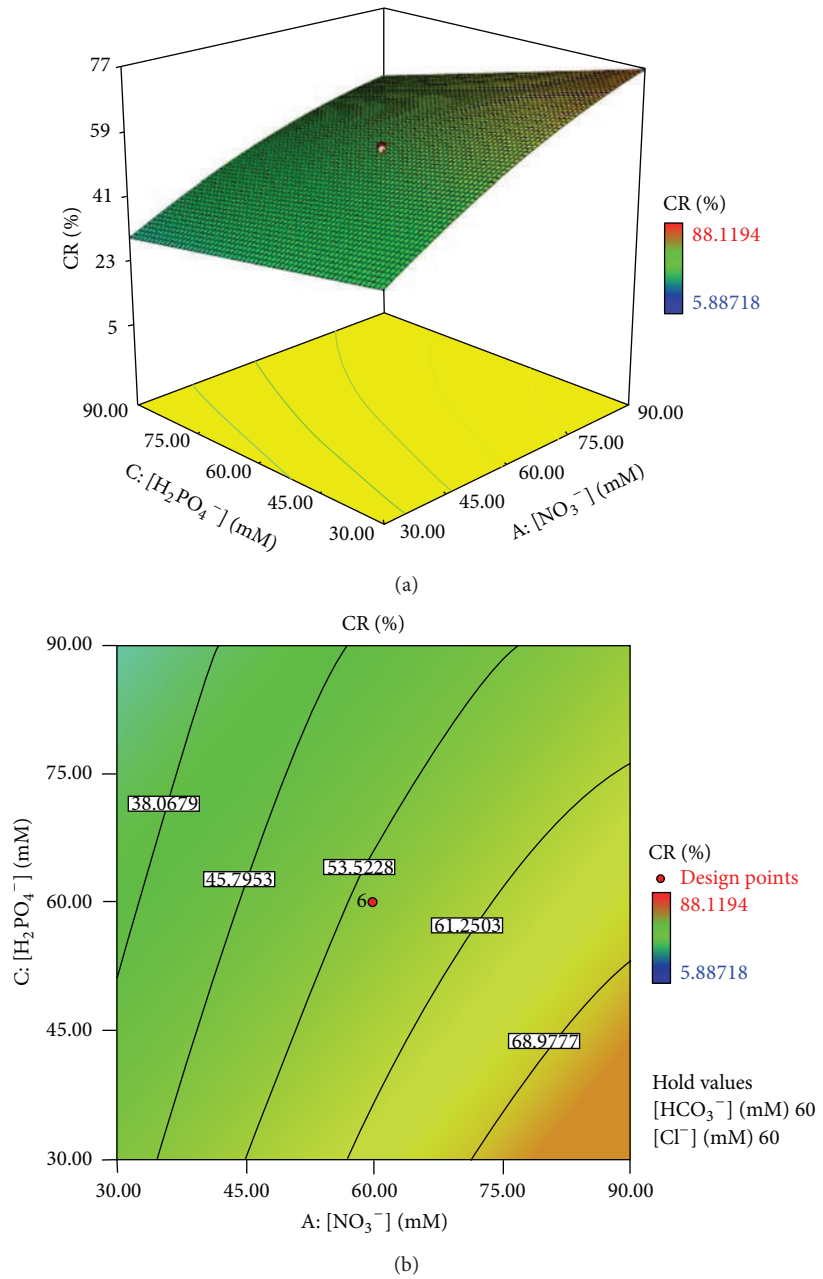

Figure 4: Response surface (a) and contour plots (b) of the removal efficiency (%) as a function of NO_3^- and $H_2PO_4^-$ concentration.

Blue 74 and indicated that the degradation efficiency of the process was enhanced with bicarbonate anion during the first 80 min of the process. This can be explained by the fact that bicarbonate ions can react with hydroxyl radicals to produce carbonate radicals, which are weak oxidizing agent [36]. The substitution of hydroxyl radicals with carbonate radicals could enhance the removal rate though less reactivity of carbonate radicals since hydroxyl radicals undergo radical-radical recombination 275 times higher than that the reaction of carbonate radicals with itself [37].

Bekbölet et al. [38] reported that the presence of phosphate ions strongly inhibited the color removal rate. The strong inhibition of $H_2PO_4^-$ ion was mainly attributed to the coagulation role of NaH_2PO_4. However, in the present study, the coagulation effect should not be an important phenomenon because TiO_2 was immobilized on glass plate. The hindering effect of $H_2PO_4^-$ can be explained by the competitive adsorption of $H_2PO_4^-$ with substance onto the surface of immobilized TiO_2. Furthermore, $H_2PO_4^-$ can react with h^+ and hydroxyl radicals to form a less reactive species, $H_2PO_4^\bullet$ [11, 12, 39].

Previous researches showed that Cl^- ions had inhibitory effects on the photocatalytic activity in slurry systems and packed-bed reactor with scavenging of hydroxyl radicals [11–13, 39]. Wang et al. [40] reported that the Cl^- ion is strongly adsorbed on the TiO_2 surface at pH 3 and reduces the removal

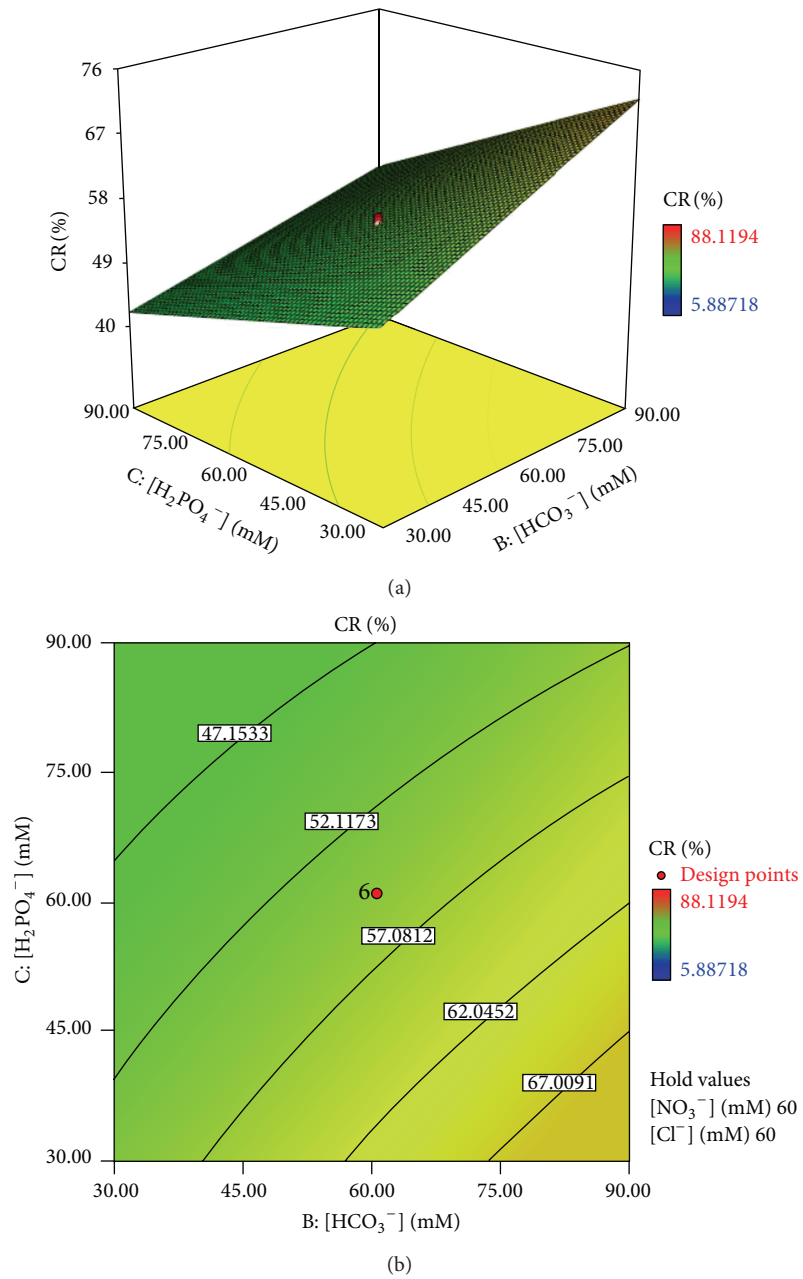

Figure 5: Response surface (a) and contour plots (b) of the removal efficiency (%) as a function of HCO_3^- and $H_2PO_4^-$ concentration.

rate whereas at neutral or alkaline conditions, the addition of the Cl^- ion did not influence the removal rate. Since attraction of the Cl^- ion by $TiOH_2^+$ and repulsion of it by TiO^- can occur at acidic and basic pH, respectively. In the present research due to the proximity of solution pH to neutral pH, this ion did not influence the removal rate.

3.4. Optimization of the Removal Efficiency Using RSM in the Presence of Various Concentrations of Inorganic Anions. RSM was used for optimization of the independent variables by the CCD model obtained from experimental data. In order to gain removal efficiency >97%, the optimum values of variables were $[NO_3^-]$ = 120 mM, $[HCO_3^-]$ = 120 mM, and $[H_2PO_4^-]$ = 0 mM. Carrying out the experiment under this optimum condition resulted in the same removal efficiency, which indicated the success and suitability of the CCD model for the optimization of the process. The removal percent obtained in a combination of NO_3^- and HCO_3^- ions with 120 mM from each shows a considerable synergy effect in comparison to a system which contains these ions individually.

The enhancement in $^{\bullet}OH$ produced in the optimized conditions can be proved with N,N-dimethyl-*p*-nitrosoaniline (RNO). This compound has absorption peak at λ_{max} = 440 nm, which reacts selectively with hydroxyl

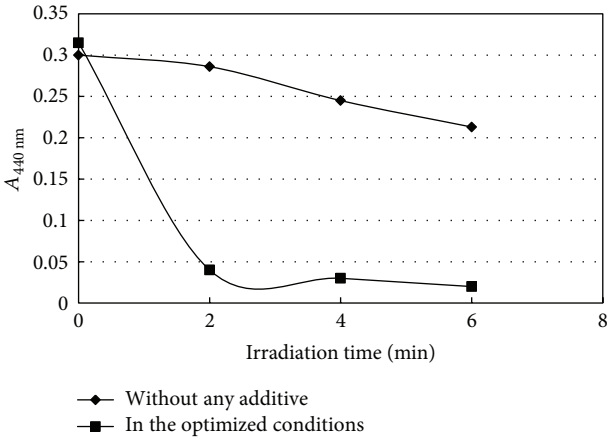

Figure 6: Changes of RNO absorbance at 440 nm versus irradiation time. $[RNO]_0 = 10^{-5}$ M.

radical but no perhydroxyl and superoxide radicals [41]. As shown in Figure 6, the absorbance of RNO at 440 nm decreased faster in the optimized conditions. This result shows that in the optimized conditions high amount of hydroxyl radicals is produced; therefore the absorption peak of RNO at $\lambda_{max} = 440$ nm decreased very faster in the presence of $[NO_3^-] = 120$ mM, $[HCO_3^-] = 120$ mM, and $[H_2PO_4^-] = 0$ mM.

4. Conclusion

Removal of organic pollutants in the fixed-bed system under UV-C irradiation can be accelerated by inorganic anions such as NO_3^- and HCO_3^- ions. The efficiency of the process depends on the inorganic anions types and concentration. The results of this study indicate that CCD methodology could be suitable for optimizing of removal process in the presence of various concentrations of inorganic anions. The NO_3^- concentration had the greatest effect and contribution in the AR17 removal whereas Cl^- ions did not have a significant effect on that. The optimal values of the NO_3^-, HCO_3^-, and $H_2PO_4^-$ concentrations were found to be 120, 120, and 0 mM, respectively. Under this condition, the highest AR17 removal percent was obtained. An important synergy effect was observed in the combination of NO_3^- and HCO_3^- ions for the removal of pollutant. Analysis of variance (ANOVA) shows a high coefficient of determination ($R^2 = 0.9866$ and $R_{adj.}^2 = 0.9822$), proving an adequate adjustment of the second-order regression model with the experimental data. In addition, it was indicated that the residuals followed a normal distribution.

Acknowledgments

The authors thank the Islamic Azad University, Tabriz Branch, and the Iranian Nanotechnology Initiative Council for financial and other means of support.

References

[1] M. A. Rauf and S. S. Ashraf, "Fundamental principles and application of heterogeneous photocatalytic degradation of dyes in solution," *Chemical Engineering Journal*, vol. 151, no. 1–3, pp. 10–18, 2009.

[2] A. R. Khataee, V. Vatanpour, and A. R. Amani Ghadim, "Decolorization of C.I. Acid Blue 9 solution by UV/Nano-TiO_2, Fenton, Fenton-like, electro-Fenton and electrocoagulation processes: a comparative study," *Journal of Hazardous Materials*, vol. 161, no. 2-3, pp. 1225–1233, 2009.

[3] N. Daneshvar, A. R. Khataee, A. R. Amani Ghadim, and M. H. Rasoulifard, "Decolorization of C.I. Acid Yellow 23 solution by electrocoagulation process: investigation of operational parameters and evaluation of specific electrical energy consumption (SEEC)," *Journal of Hazardous Materials*, vol. 148, no. 3, pp. 566–572, 2007.

[4] A. R. Khataee, "Photocatalytic removal of C.I. Basic Red 46 on immobilized TiO_2 nanoparticles: artificial neural network modelling," *Environmental Technology*, vol. 30, no. 11, pp. 1155–1168, 2009.

[5] A. Keck, J. Klein, M. Kudlich, A. Stolz, H.-J. Knackmuss, and R. Mattes, "Reduction of azo dyes by redox mediators originating in the naphthalenesulfonic acid degradation pathway of Sphingomonas sp. strain BN6," *Applied and Environmental Microbiology*, vol. 63, no. 9, pp. 3684–3690, 1997.

[6] O. Carp, C. L. Huisman, and A. Reller, "Photoinduced reactivity of titanium dioxide," *Progress in Solid State Chemistry*, vol. 32, no. 1-2, pp. 33–177, 2004.

[7] A. Fujishima, T. N. Rao, and D. A. Tryk, "Titanium dioxide photocatalysis," *Journal of Photochemistry and Photobiology C*, vol. 1, no. 1, pp. 1–21, 2000.

[8] D. Bahnemann, "Photocatalytic water treatment: solar energy applications," *Solar Energy*, vol. 77, no. 5, pp. 445–459, 2004.

[9] M. A. Fox and M. T. Dulay, "Heterogeneous photocatalysis," *Chemical Reviews*, vol. 93, no. 1, pp. 341–357, 1993.

[10] M. R. Hoffmann, S. T. Martin, W. Choi, and D. W. Bahnemann, "Environmental applications of semiconductor photocatalysis," *Chemical Reviews*, vol. 95, no. 1, pp. 69–96, 1995.

[11] C. Hu, J. C. Yu, Z. Hao, and P. K. Wong, "Effects of acidity and inorganic ions on the photocatalytic degradation of different azo dyes," *Applied Catalysis B*, vol. 46, no. 1, pp. 35–47, 2003.

[12] K. Wang, J. Zhang, L. Lou, S. Yang, and Y. Chen, "UV or visible light induced photodegradation of AO7 on TiO_2 particles: the influence of inorganic anions," *Journal of Photochemistry and Photobiology A*, vol. 165, no. 1–3, pp. 201–207, 2004.

[13] W. Zhang, T. An, M. Cui, G. Sheng, and J. Fu, "Effects of anions on the photocatalytic and photoelectrocatalytic degradation of reactive dye in a packed-bed reactor," *Journal of Chemical Technology and Biotechnology*, vol. 80, no. 2, pp. 223–229, 2005.

[14] C. Guillard, H. Lachheb, A. Houas, M. Ksibi, E. Elaloui, and J.-M. Herrmann, "Influence of chemical structure of dyes, of pH and of inorganic salts on their photocatalytic degradation by TiO_2 comparison of the efficiency of powder and supported TiO_2," *Journal of Photochemistry and Photobiology A*, vol. 158, no. 1, pp. 27–36, 2003.

[15] C. Galindo, P. Jacques, and A. Kalt, "Photodegradation of the aminoazobenzene acid orange 52 by three advanced oxidation processes: UV/H_2O_2, UV/TiO_2 and VIS/TiO_2. Comparative mechanistic and kinetic investigations," *Journal of Photochemistry and Photobiology A*, vol. 130, no. 1, pp. 35–47, 2000.

[16] S. C. R. Santos and R. A. R. Boaventura, "Adsorption modelling of textile dyes by sepiolite," *Applied Clay Science*, vol. 42, no. 1-2, pp. 137–145, 2008.

[17] A. R. Khataee, "Optimization of UV-promoted peroxydisulphate oxidation of C.I. basic blue 3 using response surface methodology," *Environmental Technology*, vol. 31, no. 1, pp. 73–86, 2010.

[18] M. A. Behnajady, N. Modirshahla, N. Daneshvar, and M. Rabbani, "Photocatalytic degradation of an azo dye in a tubular continuous-flow photoreactor with immobilized TiO_2 on glass plates," *Chemical Engineering Journal*, vol. 127, no. 1–3, pp. 167–176, 2007.

[19] A. Alinsafi, F. Evenou, E. M. Abdulkarim et al., "Treatment of textile industry wastewater by supported photocatalysis," *Dyes and Pigments*, vol. 74, no. 2, pp. 439–445, 2007.

[20] N. Daneshvar, D. Salari, A. Niaei, M. H. Rasoulifard, and A. R. Khataee, "Immobilization of TiO_2 nanopowder on glass beads for the photocatalytic decolorization of an azo dye C.I. Direct Red 23," *Journal of Environmental Science and Health A*, vol. 40, no. 8, pp. 1605–1617, 2005.

[21] M. A. Behnajady, N. Modirshahla, M. Mirzamohammady, B. Vahid, and B. Behnajady, "Increasing photoactivity of titanium dioxide immobilized on glass plate with optimization of heat attachment method parameters," *Journal of Hazardous Materials*, vol. 160, no. 2-3, pp. 508–513, 2008.

[22] S. Brown, R. Tauler, and R. Walczak, *Comprehensive Chemometrics*, vol. 1, Elsevier, Amsterdam, The Netherlands, 2009.

[23] G. E. P. Box and K. B. Wilson, "On the experimental attainment of optimum conditions," *Journal of the Royal Statistical Society B*, vol. 13, pp. 1–14, 1951.

[24] A. I. Khuri and S. Mukhopadhyay, "Response surface methodology," *Wiley Interdisciplinary Reviews*, vol. 2, no. 2, pp. 128–149, 2010.

[25] A. Aleboyeh, N. Daneshvar, and M. B. Kasiri, "Optimization of C.I. Acid Red 14 azo dye removal by electrocoagulation batch process with response surface methodology," *Chemical Engineering and Processing*, vol. 47, no. 5, pp. 827–832, 2008.

[26] M. B. Kasiri, H. Aleboyeh, and A. Aleboyeh, "Modeling and optimization of heterogeneous photo-fenton process with response surface methodology and artificial neural networks," *Environmental Science and Technology*, vol. 42, no. 21, pp. 7970–7975, 2008.

[27] http://www.imagemet.com/WebHelp/spip.htm#roughness_parameters.htm.

[28] F. Harrelkas, A. Azizi, A. Yaacoubi, A. Benhammou, and M. N. Pons, "Treatment of textile dye effluents using coagulation-flocculation coupled with membrane processes or adsorption on powdered activated carbon," *Desalination*, vol. 235, no. 1–3, pp. 330–339, 2009.

[29] H.-L. Liu and Y.-R. Chiou, "Optimal decolorization efficiency of Reactive Red 239 by UV/TiO_2 photocatalytic process coupled with response surface methodology," *Chemical Engineering Journal*, vol. 112, no. 1–3, pp. 173–179, 2005.

[30] M. S. Seyed-Dorraji, N. Daneshvar, and S. Aber, "Influence of inorganic oxidants and metal ions on photocatalytic activity of prepared zinc oxide nanocrystals," *Global Nest Journal*, vol. 11, no. 4, pp. 535–545, 2009.

[31] R. G. Zepp and N. I. Wolfe, "Abiotic transformation of organic chemicals at the particle-water interface," in *Aquatic Surface Chemistry*, pp. 423–456, John Wiley & Sons, New York, NY, USA, 1987.

[32] Z. Hua, Z. Manping, X. Zongfeng, and G. K.-C. Low, "Titanium dioxide mediated photocatalytic degradation of monocrotophos," *Water Research*, vol. 29, no. 12, pp. 2681–2688, 1995.

[33] K. Selvam, M. Muruganandham, I. Muthuvel, and M. Swaminathan, "The influence of inorganic oxidants and metal ions on semiconductor sensitized photodegradation of 4-fluorophenol," *Chemical Engineering Journal*, vol. 128, no. 1, pp. 51–57, 2007.

[34] M. Sörensen and F. H. Frimmel, "Photochemical degradation of hydrophilic xenobiotics in the UV/H_2O_2 process: influence of nitrate on the degradation rate of EDTA, 2-amino-1-naphthalenesulfonate, diphenyl-4-sulfonate and 4,4′-diaminostilbene-2,2′-disulfonate," *Water Research*, vol. 31, no. 11, pp. 2885–2891, 1997.

[35] A. Aleboyeh, M. B. Kasiri, and H. Aleboyeh, "Influence of dyeing auxiliaries on AB74 dye degradation by UV/H_2O_2process," *Journal of Environmental Management*, vol. 113, pp. 426–431, 2012.

[36] D. H. Kim and M. A. Anderson, "Solution factors affecting the photocatalytic and photoelectrocatalytic degradation of formic acid using supported TiO_2 thin films," *Journal of Photochemistry and Photobiology A*, vol. 94, no. 2-3, pp. 221–229, 1996.

[37] S. Merouani, O. Hamdaoui, F. Saoudi, M. Chiha, and C. Pétrier, "Influence of bicarbonate and carbonate ions on sonochemical degradation of Rhodamine B in aqueous phase," *Journal of Hazardous Materials*, vol. 175, no. 1–3, pp. 593–599, 2010.

[38] M. Bekbölet, Z. Boyacioglu, and B. Özkaraova, "The influence of solution matrix on the photocatalytic removal of color from natural waters," *Water Science and Technology*, vol. 38, no. 6, pp. 155–162, 1998.

[39] C. Hu, T. Yuchao, L. Lanyu, H. Zhengping, W. Yizhong, and T. Hongxiao, "Effects of inorganic anions on photoactivity of various photocatalysts under different conditions," *Journal of Chemical Technology and Biotechnology*, vol. 79, no. 3, pp. 247–252, 2004.

[40] K.-H. Wang, Y.-H. Hsieh, C.-H. Wu, and C.-Y. Chang, "The pH and anion effects on the heterogeneous photocatalytic degradation of o-methylbenzoic acid in TiO_2 aqueous suspension," *Chemosphere*, vol. 40, no. 4, pp. 389–394, 2000.

[41] K. Fukatsu and S. Kokot, "Degradation of poly(ethylene oxide) by electro-generated active species in aqueous halide medium," *Polymer Degradation and Stability*, vol. 72, no. 2, pp. 353–359, 2001.